



Published in final edited form as:

J Hazard Mater. 2016 May 5; 308: 97–105. doi:10.1016/j.jhazmat.2016.01.029.

Treatment of acid rock drainage using a sulfate-reducing bioreactor with zero-valent iron

Pedro Ayala-Parra, Reyes Sierra-Alvarez, and James A. Field*

Department of Chemical and Environmental Engineering, University of Arizona, P.O. Box 210011, Tucson, Arizona 85721, USA

Abstract

This study assessed the bioremediation of acid rock drainage (ARD) in flow-through columns testing zero-valent iron (ZVI) for the first time as the sole exogenous electron donor to drive sulfate-reducing bacteria in permeable reactive barriers. Columns containing ZVI, limestone or a mixture of both materials were inoculated with an anaerobic mixed culture and fed a synthetic ARD containing sulfuric acid and heavy metals (initially copper, and later also cadmium and lead). ZVI significantly enhanced sulfate reduction and the heavy metals were extensively removed (> 99.7%). Solid-phase analyses showed that heavy metals were precipitated with biogenic sulfide in the columns packed with ZVI. Excess sulfide was sequestered by iron, preventing the discharge of dissolved sulfide. In the absence of ZVI, heavy metals were also significantly removed (> 99.8%) due to precipitation with hydroxide and carbonate ions released from the limestone. Vertical-profiles of heavy metals in the columns packing, at the end of the experiment, demonstrated that the ZVI columns still had excess capacity to remove heavy metals, while the capacity of the limestone control column was approaching saturation. The ZVI provided conditions that enhanced sulfate reduction and generated alkalinity. Collectively, the results demonstrate an innovative passive ARD remediation using ZVI as sole electron-donor.

Keywords

Heavy Metal; Copper; Permeable reactive barrier; Anaerobic; Bioremediation

1. Introduction

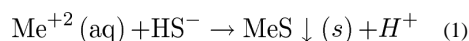
Acid rock drainage (ARD) is the effluent generated from rock residues by oxidation of metal sulfides such as pyrite (FeS_2). ARD is often characterized by low pH values (2-6), and high sulfate and heavy metals content [1, 2]. The high acidity and heavy metal concentrations typically found in ARD pose serious ecological risks, particularly for aquatic ecosystems [3, 4]. High metal levels in drinking water resources or crops impacted by ARD can also have negative impacts on human health [5-7].

Remedial approaches for ARD tend to use low cost, low maintenance passive treatments, commonly passive limestone channels and constructed wetlands [2, 8, 9]. Another passive

*Corresponding author: Tel. 1-520-621-0704, jimfield@email.arizona.edu (J. A. Field).

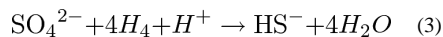
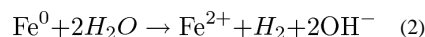
treatment option is to use permeable reactive barriers (PRB). PRB technology has been developed over the last two decades in order to provide passive, *in-situ*, treatment of groundwater. PRB is a subsurface emplacement of reactive materials through which a dissolved contaminant plume must move as it flows, typically under natural gradient [10-12]. Contaminants can be removed in PRBs by physico-chemical mechanisms (e.g., adsorption, precipitation) or microbial mechanisms. In permeable reactive biobarriers, biological activity is enhanced so that biotic processes can mediate the treatment of contaminants. PRB relying on sulfate-reducing bacteria (SRB) have been shown to be effective for the immobilization of heavy metals in ARD [13, 14].

SRB are anaerobic bacteria that utilize sulfate (SO_4^{2-}) as an electron acceptor [15]. They reduce SO_4^{2-} to sulfide (S^{2-}) utilizing H_2 and organic molecules such as lactate, pyruvate, and ethanol as electron donors (e-donor), resulting in an increase in alkalinity and pH. The biogenic sulfide produced is an excellent ligand for precipitating heavy metals. Eq. (1) illustrates how divalent metals can easily be removed in the presence of sulfide; Me stands for metal.



Sulfide minerals (MeS) are highly insoluble and can be dissolved only at highly acidic and/or strongly oxidizing conditions because their solubility constants (K_{sp}) are extremely low (Table 1). Under acidic conditions, metal sulfide precipitates are more stable than metal hydroxide and metal carbonate precipitates as indicated by their considerably higher K_{sp} constants (Table 1).

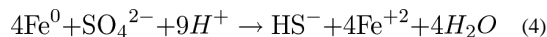
Sulfate-reducing PRBs often utilize insoluble, slow release organic substrates such as sewage, manure, compost, lignocellulosic residues, and food waste as source of carbon and an e-donor [16-18]. This work determines for the first time whether zero-valent iron (ZVI or Fe^0) can be used as a sole e-donor to generate sulfide and stimulate heavy metal removal in a flow-through bioreactor simulating a PRB system. ZVI has been shown to serve as e-donor for SRB in batch bioassays [19, 20]. However, the application of ZVI as the sole e-donating substrate in sulfate-reducing systems for heavy metal remediation has not been described to date. ZVI is readily oxidized in water under anaerobic conditions to produce H_2 . As iron is oxidized, Fe^0 produces $\text{Fe}^{2+} + 2e^-$ and H^+ is reduced to H_2 . Concomitant with the formation of H_2 is the release of OH^- (Eq. 2). SRB use the electrons via hydrogen formation to reduce sulfate (Eq. 3).



Sulfate reduction driven by abiotically formed H_2 has been demonstrated in a special culture flasks system where the abiotic corrosion of mild steel was separated from an H_2 -consuming sulfate-reducing culture except for a shared headspace [21]. However there is also evidence

for direct e-transfer from ZVI to microorganisms based on SRB accelerating the rate of ZVI corrosion beyond the abiotic rate [19, 22], evidence for involvement of c-type cytochromes in the electron transfer [23, 24], and evidence that enzymes in the cell-free-extract of a methanogen could catalyze the formation of H₂ and formate from ZVI [25].

Eq. (4), which is obtained combining Eq. (2) and (3), shows that a molar ratio of 4 moles of iron is required to reduce 1 mole of sulfate. Fe²⁺ and biogenic sulfide are produced and H⁺ is consumed, leading to an increasing the pH.



The utilization of ZVI as substrate in sulfate-reducing PRBs designed to treat ARD has the potential to provide important benefits compared to conventional organic substrates. First, ZVI is a promising strong reductant and widely available material that can drive sulfate reduction and promote the precipitation of highly stable metal sulfides. Secondly, corrosion of ZVI leads to formation of Fe²⁺ ions that can sequester excess sulfide, minimizing discharge of this toxic and malodorous contaminant into the PRB effluent. Thirdly, corrosion of ZVI consumes acidity, thereby contributing to neutralize the high acidic levels often found in ARD.

This study assessed the bioremediation of ARD in a laboratory-scale sulfate-reducing reactor using ZVI as the sole exogenous electron donor. Continuous-flow bioreactors packed with either limestone or limestone and ZVI were run in parallel to investigate the benefits of supplying limestone. The nature of the minerals deposited in the packing material of the reactors was elucidated to gain insights on the mechanisms of metal immobilization.

2. Materials and Methods

2.1. Microorganisms

Anaerobic granular sludge was obtained from an upward-flow sludge bed reactor treating brewery effluent (Mahou, Guadalajara, Spain). The sulfate-reducing activity of this sludge was demonstrated in batch experiments [26]. The sludge contained 7.13% volatile suspended solids (VSS) in wet-weight.

2.2. Chemicals

ZVI (325 mesh; 97%) was obtained from Sigma (St. Louis, MO), limestone (CaCO₃, 2-4 mm) from Oglebay Norton Industrial Sands (Buchanan, VA) and silica (2 mm) from Premier Silica (Colorado Springs, CO).

2.3. Basal medium

The basal mineral medium used to prepare the synthetic ARD contained (in mg L⁻¹): NH₄Cl (80); NaHCO₃ (50); K₂HPO₄ (171); CaCl₂·2H₂O (20), MgCl₂·6H₂O (29), yeast extract (20), and 1 mL L⁻¹ of trace element solution [20]. Copper (added as CuSO₄ 5H₂O) was gradually increased from 10 to 50 mg L⁻¹. Additional sulfate (250 mg SO₄²⁻ L⁻¹) was added as

H₂SO₄. The pH was adjusted to the desired value (see Section 2.5) by addition of NaOH or HCl.

2.4 Continuous-flow bioreactors

Three up-flow packed-bed columns (0.385 L) were inoculated with anaerobic sludge (10 g VSS L⁻¹) and operated in parallel to evaluate the removal of heavy metals using ZVI as the only exogenous source of e-donor in the presence and absence of limestone (Fig. 1). Limestone served as a pH buffer and as supplemental source of inorganic carbon for lithoautotrophic SRB that can grow using CO₂ as a sole carbon source [27]. The bioreactors were packed with sand and either ZVI (ZVI column), limestone (LS column), or limestone and ZVI (ZVI-LS column). Table 2 lists the amounts of limestone, sand and/or ZVI and anaerobic sludge supplied to each column.

The columns were operated at 30±2°C in parallel for 400 days. The feed consisted of synthetic ARD containing 250 mg SO₄²⁻ L⁻¹ and variable metal concentrations. The Cu²⁺ concentration varied from 0 to 50 mg L⁻¹ depending on the period of operation (Fig. 2). Additional heavy metals (10 mg Cd²⁺ L⁻¹ and 2.4 mg Pb²⁺ L⁻¹) were added during the final 60 days. During the initial 64 days (phase I), the influent pH was 7.2. During the next 65 days (phase II), the pH was gradually reduced from 7.2 to 3.0. Thereafter, the influent pH remained at 3.0 (phase III) (Fig. 2). The initial neutral pH conditions enabled rapid SRB enrichment. Fig. 2 shows the hydraulic retention times (HRT, calculated based on the empty-bed volume of the reactor). During the first 18 days, the reactors were operated at a HRT of approximately 1 day. From day 18 to 350, the HRT was 2 days. During the last 50 days, the HRT of the ZVI and ZVI-LS columns was 3.5 days.

Samples of the influent and effluent of the various reactors were collected regularly to determine pH, sulfide (S²⁻), SO₄²⁻, Cu²⁺, Cd²⁺ and Pb²⁺. Prior to the determination of SO₄²⁻ and soluble metals, samples were membrane filtered (0.45 µm).

2.5. Column packing characterization

2.5.1. Sequential extraction—As the experiments concluded, the packing of each column (334.5 mL) was divided into three vertical sections, each with the same volume. Sectional packing was weighed, crushed, homogenized and sampled in an anaerobic chamber to: 1) determine moisture, 2) enumerate SRB, and 3) characterize precipitates using scanning electron microscopy and energy-dispersive X-ray spectroscopy.

Copper from all sections was sequentially extracted with water, 1 M HCl, and a mixture of 16 M HNO₃-12 M HCl (3:1, v/v) following a procedure adapted from Cooper et al. [28]. A wet sample of each section (3 g) was added to 10 mL of water and vortexed for 10 min (three repetitions). Test tubes were then centrifuged (4000 rpm, 7 min) to collect the supernatant. The solids remaining were extracted with 10 mL of 1 M HCl as previously described. Finally, the remaining solid was extracted with HNO₃-HCl (3:1) in the microwave at 120°C for 35 min. The supernatant was centrifuged and collected for copper analysis.

2.5.2. Most probable number (MPN) determination—Counts of SRB were accomplished using the MPN technique [29]. Packing material (7 g wet weight) was blended in phosphate buffer (pH 7.4) and then diluted with basal medium to attain 10 mL of solution in each tube. Consecutive dilutions from 10^2 to 10^{10} fold were performed. These dilutions were incubated in a solution containing ethanol (0.01 mL/10 mL), sulfate (250 mg L^{-1}), and an iron nail. The headspace of the tubes was flushed with $\text{N}_2\text{-CO}_2$ (80-20%) for 5 min to ensure anaerobic conditions. After three weeks of incubation at room temperature, sulfate reduction was indicated by the formation of black precipitates (iron sulfide) on the iron nail.

2.5.3. Scanning electron microscopy and energy-dispersive X-ray spectroscopy (SEM-EDS)—SEM-EDS analyses were performed in a Hitachi S-4800N Type II with a cold field emission electron gun and an accelerant voltage of 20 kV. The SEM was combined with a ThermoNORAN microanalyzer for energy dispersive spectroscopy (EDS). The samples were vacuum dry and crushed to a powder material. Then, the samples were adhered to a metallic base and coated with platinum.

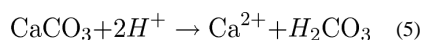
2.6. Analyses

Sulfide was analyzed colorimetrically by the methylene blue method [30]. Sulfate was measured by ion chromatography with suppressed conductivity using an AS11-HC4 column (Dionex, Sunnydale, CA) and a conductivity detector. Copper was determined by inductively coupled plasma-optical emission spectrometry (2100 Optima ICP-OES, Perkin Elmer, Waltham, MA). Wavelengths used for Cu^{2+} , Pb^{2+} and Cd^{2+} determinations were: 327.3, 220.3 and 228.8 nm, respectively. VSS and pH were determined according to standard methods [31].

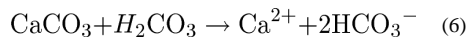
3. Results and Discussion

3.1. pH evolution

During phase I, the effluent pH increased to 9 and 10 in the two ZVI reactors, whereas the effluent pH remained neutral in the case of the LS column (Fig. 3). In phases II and III, as the influent pH decreased from 7.2 to 3.0, the effluent of the three columns was neutral to mildly alkaline. From day 250 and beyond, all effluents had similar pH values, between 7.2 and 7.7. The effluent of the LS column usually had a lower pH compared to the effluent of the ZVI-containing columns. The three columns were able to handle very low pH values, which are common in ARD, and increased the pH of the effluent to the circumneutral values typically required by SRB [32]. The increase in the pH of the effluent of the LS column was primarily due to the release of bicarbonate alkalinity from the limestone packing which is beneficial for acid neutralization and pH buffering. In acidic waters (pH less than 6.4), limestone reacts according to the following reaction [33]:



H_2CO_3 continues to react with limestone according to the following reaction:



In ZVI-amended columns, alkalinity can be generated by anoxic corrosion of ZVI (Eq. 2) and sulfate reduction (Eq. 3), as both processes involve the consumption of H^+ .

3.2. Sulfate reduction

Previous reports indicate that ZVI corrosion can provide electrons via H_2 to stimulate microbial sulfate reduction [19, 20]. Based on (Eq. 4), 4 mol of ZVI are required to reduce 1 mol of SO_4^{2-} . The ZVI reactors were supplied with 183.4 g ZVI, which is 5.5-fold higher than the theoretical amount needed to reduce the cumulative amount of SO_4^{2-} supplied (14.3 g). These calculations are based on an HRT of 2 d (0.19 L d^{-1}) and $250 \text{ mg SO}_4^{2-} \text{ L}^{-1}$ over one year of operation.

Fig. 4 shows sulfate removal efficiency differences between the ZVI and ZVI-LS reactors. During phase I, the ZVI reactors achieved sulfate removal efficiencies ranging from 40 to 50%; the best performance was achieved by the ZVI-LS column. In phase II, both columns removed sulfate as in phase I. In most of phase II and through period (e_1) of phase III, there was a slightly improved performance by ZVI-LS compared to the ZVI column. The ZVI-LS column was approximately 10% more efficient than the ZVI reactor over phases I and II. During phase III, the ZVI-LS reactor was around 30% more efficient during periods (b) and (c), and 65% more efficient over periods (d) and (e_1). In phase III period (e_2), the sulfate reduction efficiency of the ZVI column was the same as the ZVI-LS. The better performance of ZVI-LS compared to ZVI column could be due to the improved inorganic carbon supply in the former. Some SRB are chemolithoautrophic utilizing CO_2 as carbon source [27].

At the beginning of phase III, sulfate removal decreased to 25% and 35% in the ZVI and ZVI-LS columns, respectively, due to the drop in influent pH from 7.2 to 3.0. The subsequent recovery of sulfate reduction was possibly due to an increase in the SRB population. Later, in phase III period (e_2), when the HRT of the ZVI columns was increased from 2.0 to 3.5 days, the sulfate removal efficiency reached 50%. The high sulfate reduction rates maintained after 400 d of operation indicate that the e-donor capacity of ZVI was not exhausted.

During phase I, the LS column achieved a sulfate removal of only 10%. The removal efficiency decreased to 5% in phase II and ceased at the beginning of phase III. Sulfate reduction in the LS column was driven by endogenous substrate derived from the decay of the inoculum, and lasted until the biomass decomposition was exhausted. A previous study showed that the inoculum used in this study had measurable endogenous e-donor contribution [34].

Soluble copper is known to inhibit SRB but the reported 50% inhibitory concentrations range drastically from only 0.84 mg L^{-1} to greater than 763 mg L^{-1} [35-38]. In this study, copper was supplied at concentrations between 10 and 50 mg L^{-1} . Fig. 4 shows that the sulfate removal efficiency of the ZVI columns was similar in periods (c), (d), (e_1) and (e_2), regardless of the copper concentration in the influent. The observation that the presence of

Cu^{2+} in the influent had no measurable impact on inhibiting sulfate reduction is consistent with the sharp decrease in the Cu^{2+} concentration attained by the ZVI columns, as will be discussed later in Section 3.4. Previous studies have shown attenuation of copper toxicity by biogenic sulfide [26]. The apparent increase in the sulfate removal efficiency in the last period of operation (e_2 , in Fig. 4), when the HRT was increased from 2.0 to 3.5 d, does not imply recovery from toxicity since the volumetric removal rate of sulfate remained the same as in the previous period (Fig. 4B).

SRB were enumerated in the packing of the various columns at the end of the experiment. The SRB count in the methanogenic inoculum was very low ($101 \text{ cells g}^{-1} \text{ dwt}$). Continuous operation of the various reactors for 400 days with a sulfate-containing feed led to a marked increase in the SRB counts. Whereas the lowest SRB count was in the in the bottom section of the LS column ($4.5 \times 10^5 \text{ cells g}^{-1} \text{ dry packing}$), the SRB counts were highest in the bottom sections of the ZVI-LS and ZVI columns, 3.8×10^7 and $2.7 \times 10^7 \text{ cells g}^{-1} \text{ dry packing}$, respectively. The 60 to 85-fold higher SRB counts in the ZVI-amended reactors indicate that ZVI served as e-donor of the growth of the SRB population. Isotopic evidence from a previous study also demonstrated that ZVI enhanced sulfate reduction in biologically active columns [39]. The slightly improved performance in the ZVI-LS column versus the ZVI column may be due to its slightly higher SRB population.

3.3. Sequestration of biogenic sulfide

Biogenic sulfide may be captured in the bioreactors due to the formation of metal sulfides. Fig. 5 shows the concentration of sulfide in the effluent of the bioreactors as a function of time. Sulfide was detected in the effluent of the LS column in phases I, II and the first part of phase III, indicating microbial sulfate reduction (Fig. 5). Since the LS column did not receive an exogenous e-donor, microbial sulfate reduction was sustained by the endogenous substrate in the inoculum biomass. However, after 90 days of operation a sharp decrease in the concentration of sulfide released by the LS column was observed, most likely due to gradual depletion of the endogenous substrate in the inoculum. On the other hand, the ZVI and ZVI-LS columns discharged very little or no sulfide, despite these columns having much greater levels of sulfate reduction compared to the LS column (Fig. 5). Thus, the sulfide generated in the ZVI columns was for the most part sequestered in the column due to reaction with Fe^{2+} (periods a, d), or Fe^{2+} plus Cu^{2+} (during periods b, c and e). The effectiveness of ZVI to decrease the concentration of sulfide discharged in the effluent is illustrated in Fig. 6, which shows the $\text{S}^{2-}\text{-S}$ sequestered, *i.e.*, the difference between the concentration of $\text{SO}_4^{2-}\text{-S}$ removed and $\text{S}^{2-}\text{-S}$ discharged by the various columns, during two different periods of operation, with no copper addition (Fig. 6A) and with addition of $10 \text{ mg Cu}^{+2} \text{ L}^{-1}$ (Fig. 6B). The sulfide levels in the effluent of the columns amended with ZVI was very low indicating extensive sequestration of the biogenic sulfide in the columns.

3.4. Removal of Cu, Cd and Pb

The concentration of soluble copper in the effluent of the three columns was always lower than $70 \mu\text{g L}^{-1}$ (Fig. 7). All reactors demonstrated very high copper removal efficiencies ranging from 99.8 to 99.9%, even during the period when the feed contained copper concentrations as high as 50 mg L^{-1} . Bai and coworkers [40] also treated ARD in a high-

rate SRB bioreactor using ZVI and lactate as e-donors and attained Cu^{2+} removal efficiencies up to 99%. However, in contrast with our study, Bai used an organic substrate as the main e-donor source. Furthermore, the excellent treatment effectiveness obtained in the limestone columns are in agreement with several studies that demonstrate effective removal of heavy metals by using limestone channels via adsorption or precipitation [41, 42].

Metal-sulfide precipitation is the main mechanism expected to contribute to the removal of copper in the ZVI-amended columns. In the presence of biogenic sulfide, copper sulfide is formed due to the considerably lower K_{sp} value of CuS compared to $\text{Cu}(\text{OH})_2$ and CuCO_3 (Table 1). In this sense, it is interesting to note that Sierra-Alvarez and coworkers [43] reported that the predominant copper sulfide mineral formed in a sequential sulfate-reducing bioreactor-crystallization reactor was covellite. The concentration of biogenic sulfide in the ZVI columns exceeded the stoichiometry requirement for the quantitative precipitation of the copper added. Considering the stoichiometry of CuS , 25.2 mg L^{-1} of sulfide is needed to precipitate the highest concentration of copper added (50 mg L^{-1}). When the columns were fed 50 mg L^{-1} copper, the average sulfate removal in both ZVI columns was $79.4 \text{ mg SO}_4^{2-} \text{ L}^{-1}$, which is equivalent to 26.4 mg L^{-1} of S^{2-} produced. Thus, there was sufficient sulfide to assure that all the added Cu^{2+} could be sequestered in the columns as CuS . It should be noted that although sulfate reduction is the main process generating sulfide, FeS could also potentially immobilize heavy metals. Fe^{+2} in FeS can be displaced by divalent metals with more affinity for S^{2-} . For example, copper and cadmium will form metal sulfides with FeS while Fe^{2+} is released in the aqueous phase [44].

Biogenic sulfide also contributed to the removal of copper during the early stages of operation of the LS column. However, from period (c) onwards, the LS column was no longer reducing sulfate (Fig. 5), thus copper immobilization was likely mediated by precipitation with hydroxide and carbonate ions released from limestone (CaCO_3) dissolution. Solid phase analysis of Cu reacting with limestone (CaCO_3) in previous studies has provided evidence for CuCO_3 formation and its adsorption on calcite surfaces [45, 46]. The main advantages of using limestone are low costs and high efficiency of metal removal. The disadvantage is that rock surfaces are saturated after a short time period [47, 48].

In period (e₂), soluble Pb^{2+} (10.0 mg L^{-1}) and Cd^{2+} (2.4 mg L^{-1}) were added to the influent, in addition to Cu^{2+} . The effluent concentrations of Cd and Pb in all the columns were very low, averaging 17 and $11 \text{ } \mu\text{g L}^{-1}$, respectively (Fig. 8). Sulfate reduction in the LS column was negligible during this period (Fig. 4) suggesting that metal immobilization was due to carbonate and hydroxide precipitation. The solubility of Cd^{2+} and Pb^{2+} sulfides is extremely low (Table 2) and, therefore, Cd and Pb were most likely retained as metal sulfides in the sulfate-reducing bioreactors. The amount of sulfide required to precipitate $50 \text{ mg Cu}^{2+} \text{ L}^{-1}$, $10 \text{ mg Cd}^{2+} \text{ L}^{-1}$ and $2.4 \text{ mg Pb}^{2+} \text{ L}^{-1}$ would be 25.2 , 2.84 and 0.37 mg L^{-1} , respectively; requiring a total sulfide of 28.4 mg L^{-1} . The average sulfate removal in the ZVI-amended columns was 40%, corresponding to reduction of 100 mg SO_4^{2-} and the concomitant generation of 33.3 mg L^{-1} of sulfide (Fig. 4), thus assuring a 17% excess of sulfide. Other studies have also reported that the main mechanism of Cu^{2+} , Cd^{2+} and Pb^{2+} removal in sulfate-reducing bioreactors is precipitation in the form of metal sulfides [43, 49-51].

3.5. Packing material characterization and mechanisms of metal removal

Packing material from each column was collected and extracted sequentially to assess the amount and nature of the copper retained in the columns. The total amount of copper recovered from the column packing was quite high, ranging from 84 to 93% of the cumulative copper removed from the effluent (Table 3). Most of the copper in the LS column was extracted with 1 M HCl, which is consistent with the high solubility constant of $\text{Cu}(\text{OH})_2$ and CuCO_3 . In contrast, 1 M HCl was ineffective in extracting copper from the ZVI-containing columns. However, concentrated HNO_3 -HCl extracted a large fraction of the copper from the ZVI columns, indicating that the precipitated copper was more stable and distinct from copper carbonates or hydroxides expected in the LS column. These results suggest that the copper minerals in the ZVI columns consisted of copper sulfide. This hypothesis is supported by laboratory experiments performed by Cooper and coworkers [28] confirming that sulfide minerals of copper such as covellite (CuS) and chalcocite (Cu_2S) are predominantly extracted by HNO_3 and not HCl. The formation of copper sulfide under sulfate reducing conditions is also consistent with the considerably lower K_{sp} of CuS compared to $\text{Cu}(\text{OH})_2$ and CuCO_3 (Table 1). Numerous sulfate-reducing studies have demonstrated that biogenic sulfide is an excellent ligand of different heavy metals, including Cu^{2+} , with a high tendency to form poorly soluble metal sulfides [43, 52, 53]. It is possible that corrosion products on the ZVI surface could have contributed to adsorb or co-precipitate some Cu^{2+} , but based on the sequential extraction data (Table 3) this does not seem to be the dominant removal mechanism. As shown on Table 3, only a small fraction of the copper removed in the reactors amended with ZVI could be extracted with HCl.

The bottom and mid-sections of the LS column contained relatively similar concentrations of copper, and the top section had about half the copper concentration as the lower two sections (Table 3). These results suggest that, by the end of the experiment, the capacity of the LS column to sequester copper was partially depleted. In contrast, in the ZVI and ZVI-LS columns most of the copper was immobilized in the bottom section of the reactors indicating that both columns still had significant capacity to sequester copper even after 400 days of continuous operation at HRTs ranging from 1 to 3.3 days. Much longer service times would be expected in practice since typical HRT values in operating PRB are considerably longer. For example, Barlett and Morrison [54] determined that the residence time in two different locations of a full-scale PRB averaged 16.4 and 22.3 days. Field-scale application of iron-based technologies for the remediation of contaminated groundwater has shown promising results over relatively long treatment periods (e.g. up to ten years, [55]).

XRD and SEM-EDS measurements were performed to reveal the predominant elements in the columns. Unfortunately, XRD analysis did not provide conclusive evidence about the nature of the copper minerals due to interferences by the high concentrations of sand and calcite (limestone) and/or iron minerals with greater crystallinity in the various columns. SEM-EDS analyses on the other hand revealed that copper was an abundant element, along with calcium, in the packing of the LS column (Fig. 9). In contrast, Fe was the most abundant element in the ZVI columns, but copper was also present. The elemental composition of the ZVI packing material was measured along a trajectory transecting a precipitate aggregate. The background in the transect line analysis is mainly iron (dark gray

area in the SEM). As the transect moves into the center of the precipitate microstructure (white area), the relative abundance of sulfur and copper increases as iron decreases. The molar ratio of Cu:S determined (1:1.04) suggests that CuS constituted the main mineral in the precipitate. These results, combined with the copper and sulfur balances (Table 3, Fig. 6), convincingly show that SRB activity was responsible for the effective removal of copper in the ZVI containing columns.

4. Conclusions

The results obtained demonstrate that ZVI can serve as the sole exogenous slow-release electron donor to drive sulfate reduction over an extended time period in continuous-flow laboratory-scale columns treating a synthetic ARD containing high heavy metal concentrations (up to 50 mg/L of copper) and pH values ranging from 3.0 to 7.0. Treatment of this synthetic ARD was feasible and provided very high removal efficiencies of copper, cadmium and lead (> 99.7%) and pH increase to circumneutral values (7.3-7.7) for over 400 days of operation at short HRTs (1-3 days). Moreover, the use of ZVI resulted in very low concentrations of toxic, malodorous hydrogen sulfide in the effluent due to its effective precipitation as metal sulfides, including sulfides of Fe²⁺ released from anoxic corrosion of ZVI. Element microanalysis and thermodynamic calculations using solubility products constants indicated that formation of insoluble metal sulfides was responsible for the effective metal removal in the ZVI columns. Continuous treatment of the synthetic ARD in a column packed with limestone also provided effective metal removal and acidity consumption. However, limestone did not contribute to sulfate reduction or to sequester biogenic sulfide and its treatment capacity had a lower longevity compared to ZVI. These results indicate that ZVI is a promising reactive material for the treatment of ARD in sulfate-reducing PRB systems.

Acknowledgements

Funding was received from the National Institute of Environment and Health Sciences-supported Superfund Research Program (NIH ES-04940). Ayala-Parra was supported by the Mexican National Council of Science and Technology.

References

- [1]. Nordstrom DK. Baseline and premining geochemical characterization of mined sites. *Appl. Geochem.* 2015; 57:17–34.
- [2]. Akcil A, Koldas S. Acid mine drainage (AMD): causes, treatment and case studies. *J. Clean. Prod.* 2006; 14:1139–1145.
- [3]. Byrne P, Wood PJ, Reid I. The impairment of river systems by metal mine contamination: A review including remediation options. *Crit. Rev. Env. Sci. Tec.* 2012; 42:2017–2077.
- [4]. DeNicol DM, Stapleton MG. Impact of acid mine drainage on benthic communities in streams: the relative roles of substratum vs. aqueous effects. *Environ. Pollut. (Barking, Essex : 1987).* 2002; 119:303–315.
- [5]. Cobb GP, Sands K, Waters M, Wixson BG, Dorward-King E. Accumulation of heavy metals by vegetables grown in mine wastes. *Environ. Toxicol. Chem.* 2000; 19:600–607.
- [6]. Sharma RK, Agrawal M. Biological effects of heavy metals: An overview. *J. Environ. Biol.* 2005; 26:301–313. [PubMed: 16334259]
- [7]. Williams M. Arsenic in mine waters: an international study. *Environ. Geol.* 2001; 40:267–278.

- [8]. Johnson DB, Hallberg KB. Acid mine drainage remediation options: a review. *Sci. Total Environ.* 2005; 338:3–14. [PubMed: 15680622]
- [9]. Ziemkiewicz PF, Skousen JG, Brant DL, Sterner PL, Lovett RJ. Acid mine drainage treatment with armored limestone in open limestone channels. *J. Environ. Qual.* 1997; 26:1017–1024.
- [10]. Obiri-Nyarko F, Grajales-Mesa SJ, Malina G. An overview of permeable reactive barriers for in situ sustainable groundwater remediation. *Chemosphere.* 2014; 111:243–259. [PubMed: 24997925]
- [11]. Richardson JP, Nicklow JW. In situ permeable reactive barriers for groundwater contamination. *Soil Sediment Contam.* 2002; 11:241–268.
- [12]. Scherer MM, Richter S, Valentine RL, Alvarez PJ. Chemistry and microbiology of permeable reactive barriers for in situ groundwater clean up. *Crit. Rev. Microbiol.* 2000; 26:221–264. [PubMed: 11192023]
- [13]. Neculita CM, Zagury GJ, Bussiere B. Passive treatment of acid mine drainage in bioreactors using sulfate-reducing bacteria: Critical review and research needs. *J. Environ. Qual.* 2007; 36:1–16. [PubMed: 17215207]
- [14]. Gibert O, de Pablo J, Cortina JL, Ayora C. Treatment of acid mine drainage by sulphate-reducing bacteria using permeable reactive barriers: A review from laboratory to full-scale experiments. *Re/Views Environ. Sci. Bio/Technol.* 2002; 1:327–333.
- [15]. Dar SA, Kleerebezem R, Stams AJM, Kuenen JG, Muyzer G. Competition and coexistence of sulfate-reducing bacteria, acetogens and methanogens in a lab-scale anaerobic bioreactor as affected by changing substrate to sulfate ratio. *Appl. Microbiol. Biot.* 2008; 78:1045–1055.
- [16]. Gibert O, Rotting T, Cortina JL, de Pablo J, Ayora C, Carrera J, Bolzicco J. In-situ remediation of acid mine drainage using a permeable reactive barrier in Aznalcollar (Sw Spain). *J. Hazard. Mater.* 2011; 191:287–295. [PubMed: 21601356]
- [17]. Cocos IA, Zagury GJ, Clement B, Samson R. Multiple factor design for reactive mixture selection for use in reactive walls in mine drainage treatment. *Water Res.* 2002; 36:167–177. [PubMed: 11766792]
- [18]. Tsukamoto TK, Killion HA, Miller GC. Column experiments for microbiological treatment of acid mine drainage: low-temperature, low-pH and matrix investigations. *Water Res.* 2004; 38:1405–1418. [PubMed: 15016517]
- [19]. Dinh HT, Kuever J, Mussmann M, Hassel AW, Stratmann M, Widdel F. Iron corrosion by novel anaerobic microorganisms. *Nature.* 2004; 427:829–832. [PubMed: 14985759]
- [20]. Karri S, Sierra-Alvarez R, Field JA. Zero valent iron as an electron-donor for methanogenesis and sulfate reduction in anaerobic sludge. *Biotechnol. Bioeng.* 2005; 92:810–819. [PubMed: 16136594]
- [21]. Rajagopal BS, Legall J. Utilization of cathodic hydrogen by hydrogen-oxidizing bacteria. *Appl. Microbiol. Biot.* 1989; 31:406–412.
- [22]. Venzlaff H, Enning D, Srinivasan J, Mayrhofer KJJ, Hassel AW, Widdel F, Stratmann M. Accelerated cathodic reaction in microbial corrosion of iron due to direct electron uptake by sulfate-reducing bacteria. *Corros. Sci.* 2013; 66:88–96.
- [23]. Beese-Vasbender PF, Nayak S, Erbe A, Stratmann M, Mayrhofer KJJ. Electrochemical characterization of direct electron uptake in electrical microbially influenced corrosion of iron by the lithoautotrophic SRB *Desulfopila corrodens* strain IS4. *Electrochim. Acta.* 2015; 167:321–329.
- [24]. Strycharz SM, Glaven RH, Coppi MV, Gannon SM, Perpetua LA, Liu A, Nevin KP, Lovley DR. Gene expression and deletion analysis of mechanisms for electron transfer from electrodes to *Geobacter sulfurreducens*. *Bioelectrochem.* 2011; 80:142–150.
- [25]. Deutzmann JS, Sahin M, Spormann AM. Extracellular enzymes facilitate electron uptake in biocorrosion and bioelectrosynthesis. *Mbio.* 2015; 6
- [26]. Gonzalez-Estrella J, Puyol D, Sierra-Alvarez R, Field JA. Role of biogenic sulfide in attenuating zinc oxide and copper nanoparticle toxicity to acetoclastic methanogenesis. *J. Hazard. Mater.* 2015; 283:755–763. [PubMed: 25464319]

- [27]. Brysch K, Schneider C, Fuchs G, Widdel F. Lithoautotrophic growth of sulfate-reducing bacteria, and description of *Desulfobacterium-autotrophicum* gen-nov, sp-nov. Arch. Microbiol. 1987; 148:264–274.
- [28]. Cooper DC, Morse JW. Extractability of metal sulfide minerals in acidic solutions: Application to environmental studies of trace metal contamination within anoxic sediments. Environ. Sci. Technol. 1998; 32:1076–1078.
- [29]. Fedorak PM, Semple KM, Westlake DWS. A statistical comparison of 2 culturing methods for enumerating sulfate-reducing bacteria. J. Microbiol. Meth. 1987; 7:19–27.
- [30]. Truper HG, Schlegel HG. Sulphur metabolism in Thiorhodaceae .1. quantitative measurements on growing cells of *Chromatium okenii*. Anton. Van Lee. J. M. S. 1964; 30:225–238.
- [31]. APHA. Standard Methods for the Examination of Water and Wastewater. APHA, AWWA and WEF; Washington D.C.: 1999.
- [32]. Hao OJ, Chen JM, Huang L, Buglass RL. Sulfate-reducing bacteria. Crit. Rev. Env. Sci. Tec. 1996; 26:155–187.
- [33]. Gazea B, Adam K, Kontopoulos A. A review of passive systems for the treatment of acid mine drainage. Miner. Eng. 1996; 9:23–42.
- [34]. Tapia-Rodriguez A, Luna-Velasco A, Field JA, Sierra-Alvarez R. Anaerobic bioremediation of hexavalent uranium in groundwater by reductive precipitation with methanogenic granular sludge. Water Res. 2010; 44:2153–2162. [PubMed: 20060558]
- [35]. Utgikar VP, Chen BY, Chaudhary N, Tabak HH, Haines JR, Govind R. Acute toxicity of heavy metals to acetate-utilizing mixed cultures of sulfate-reducing bacteria: EC100 and EC50. Environ. Toxicol. Chem. 2001; 20:2662–2669. [PubMed: 11764146]
- [36]. Hsu HF, Kumar M, Ma YS, Lin JG. Extent of precipitation and sorption during copper removal from synthetic wastewater in the presence of sulfate-reducing bacteria. Environ. Eng. Sci. 2009; 26:1087–1096.
- [37]. Karri S, Sierra-Alvarez R, Field JA. Toxicity of copper to acetoclastic and hydrogenotrophic activities of methanogens and sulfate reducers in anaerobic sludge. Chemosphere. 2006; 62:121–127. [PubMed: 15936054]
- [38]. Sani RK, Peyton BM, Brown LT. Copper-induced inhibition of growth of *Desulfovibrio desulfuricans* G20: Assessment of its toxicity and correlation with those of zinc and lead. Appl. Environ. Microbiol. 2001; 67:4765–4772. [PubMed: 11571183]
- [39]. Kumar N, Millot R, Battaglia-Brunet F, Negrel P, Diels L, Rose J, Bastiaens L. Sulfur and oxygen isotope tracing in zero valent iron based In situ remediation system for metal contaminants. Chemosphere. 2013; 90:1366–1371. [PubMed: 23000047]
- [40]. Bai H, Kang Y, Quan H, Han Y, Sun J, Feng Y. Treatment of acid mine drainage by sulfate reducing bacteria with iron in bench scale runs. Bioresource Technol. 2013; 128:818–822.
- [41]. Alcolea A, Vazquez M, Caparros A, Ibarra I, Garcia C, Linares R, Rodriguez R. Heavy metal removal of intermittent acid mine drainage with an open limestone channel. Miner. Eng. 2012; 26:86–98.
- [42]. Sdiri A, Bouaziz S. Re-evaluation of several heavy metals removal by natural limestones. Front. Chem. Sci. Eng. 2014; 8:418–432.
- [43]. Sierra-Alvarez R, Hollingsworth J, Zhou MS. Removal of copper in an integrated sulfate reducing bioreactor-crystallization reactor system. Environ. Sci. Technol. 2007; 41:1426–1431. [PubMed: 17593752]
- [44]. Peng J-F, Song Y-H, Yuan P, Cui X-Y, Qiu G-L. The remediation of heavy metals contaminated sediment. J. Hazard. Mater. 2009; 161:633–640. [PubMed: 18547718]
- [45]. Cravotta CA, Trahan MK. Limestone drains to increase pH and remove dissolved metals from acidic mine drainage. Appl. Geochem. 1999; 14:581–606.
- [46]. Fronczyk J, Radziemska M, Mazur Z. Copper removal from contaminated groundwater using natural and engineered limestone sand in permeable reactive barriers. Fresenius Environ. Bull. 2015; 24:228–234.
- [47]. Cravotta CA III. Laboratory and field evaluation of a flushable oxic limestone drain for treatment of net-acidic drainage from a flooded anthracite mine, Pennsylvania, USA. Appl. Geochem. 2008; 23:3404–3422.

- [48]. Huminicki DMC, Rimstidt JD. Neutralization of sulfuric acid solutions by calcite dissolution and the application to anoxic limestone drain design. *Appl. Geochem.* 2008; 23:148–165.
- [49]. Gomez DKV, Enright AM, Rini EL, Buttice A, Kramer H, Lens P. Effect of hydraulic retention time on metal precipitation in sulfate reducing inverse fluidized bed reactors. *J. Chem. Technol. Biotechnol.* 2015; 90:120–129.
- [50]. Song Y, Fitch M, Burken J, Nass L, Chilukiri S, Gale N, Ross C. Lead and zinc removal by laboratory-scale constructed wetlands. *Water Environ. Res.* 2001; 73:37–44. [PubMed: 11558300]
- [51]. Velasco A, Ramirez M, Volke-Sepulveda T, Gonzalez-Sanchez A, Revah S. Evaluation of feed COD/sulfate ratio as a control criterion for the biological hydrogen sulfide production and lead precipitation. *J. Hazard. Mater.* 2008; 151:407–413. [PubMed: 17640800]
- [52]. Sahinkaya E, Gungor M, Bayrakdar A, Yucesoy Z, Uyanik S. Separate recovery of copper and zinc from acid mine drainage using biogenic sulfide. *J. Hazard. Mater.* 2009; 171:901–906. [PubMed: 19608339]
- [53]. Cao X, Cao H, Sheng Y, Xie Y, Zhang K, Zhang Y, Crittenden JC. Mechanisms of Cu²⁺ migration, recovery and detoxification in Cu²⁺-, SO₄²⁻-containing wastewater treatment process with anaerobic granular sludge. *Environ. Technol.* 2014; 35:1956–1961. [PubMed: 24956789]
- [54]. Bartlett TR, Morrison SJ. Tracer method to determine residence time in a permeable reactive barrier. *Ground Water.* 2009; 47:598–604. [PubMed: 19245377]
- [55]. Phillips DH, Van Nooten T, Bastiaens L, Russell MI, Dickson K, Plant S, Ahad JM, Newton T, Elliot T, Kalin RM. Ten year performance evaluation of a field-scale zero-valent iron permeable reactive barrier installed to remediate trichloroethene contaminated groundwater. *Environ. Sci. Technol.* 2010; 44:3861–3869. [PubMed: 20420442]
- [56]. Blais JF, Djedidi Z, Cheikh RB, Tyagi RD, Mercier G. Metals precipitation from effluents: Review. *Pract. Period. Hazard. Toxic Radioact. Waste Manage.* 2008; 12:135–149.

Highlights

- Electron donor from zero-valent iron (ZVI) drives sulfate reduction to sulfide.
- Sulfide converts soluble heavy metals into sulfide minerals.
- Excess sulfide is sequestered by iron preventing discharge.
- Corrosion of ZVI consumes acidity in acid rock drainage.
- ZVI as reactive material outlasted limestone in removing heavy metals.

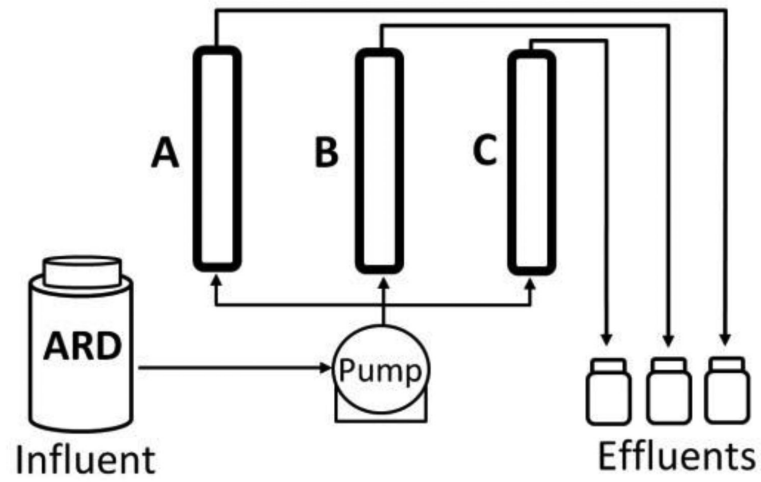


Fig. 1. Diagram of the packed-bed columns used in this study. A) Column packed with limestone (LS), B) column packed with ZVI and limestone (ZVI-LS) column, and C) column packed with ZVI (ZVI).

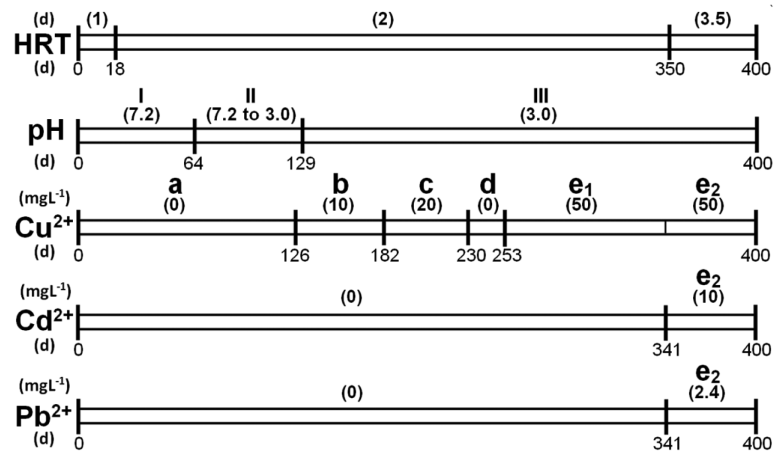


Fig. 2.

Diagram illustrating the conditions maintained in each phase and period of column operation. The phases of the experiment (I, II, and III) are defined by the pH regimen. The periods of the experiment (a, b, c, d, e₁ and e₂) are defined by the heavy metal additions.

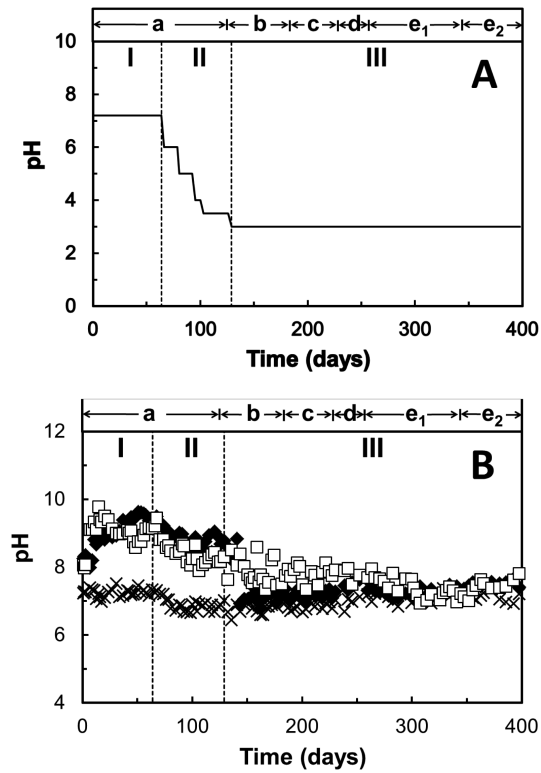


Fig. 3. Influent pH (A) and effluent pH (B) during three separate periods of reactor operation with influent adjusted to pH values of: 7.2 (period I), from 7.2 to 3.0 (period II) and 3.0 (period III). Columns: ZVI-LS (◆), ZVI (□), and LS (×). The periods of the experiment are defined by the heavy metal additions as indicated in Fig. 2.

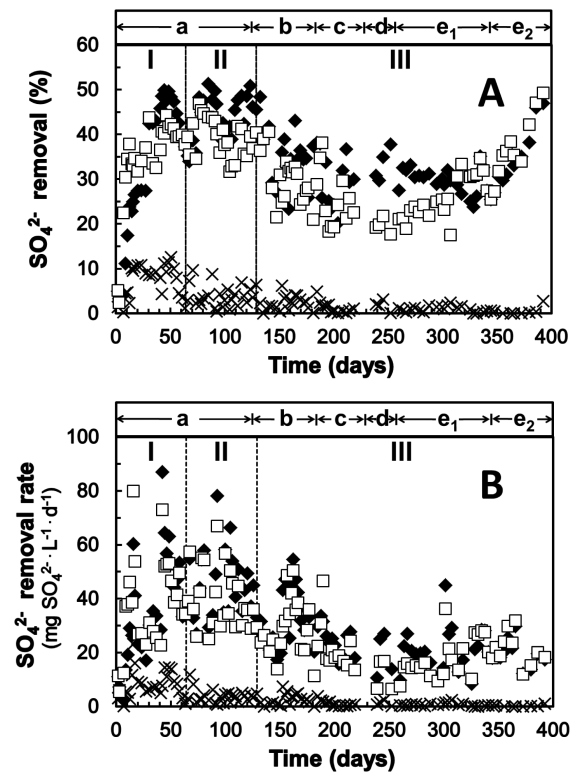


Fig. 4. Sulfate removal efficiency (A) and volumetric sulfate removal (B) during the operation of the ZVI-LS column (◆), ZVI column (□), and LS column (×). The conditions of operation during the various phases of the experiment are defined in Fig. 2.

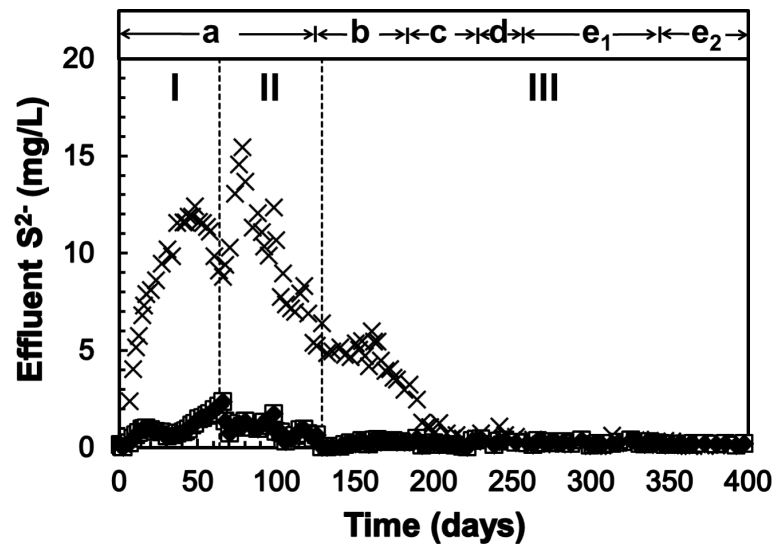


Fig. 5. Effluent sulfide concentration during the operation of the ZVI-LS column (\blacklozenge), ZVI column (\square), and LS column (\times). The conditions of operation during the various phases of the experiment are defined in Fig. 2.

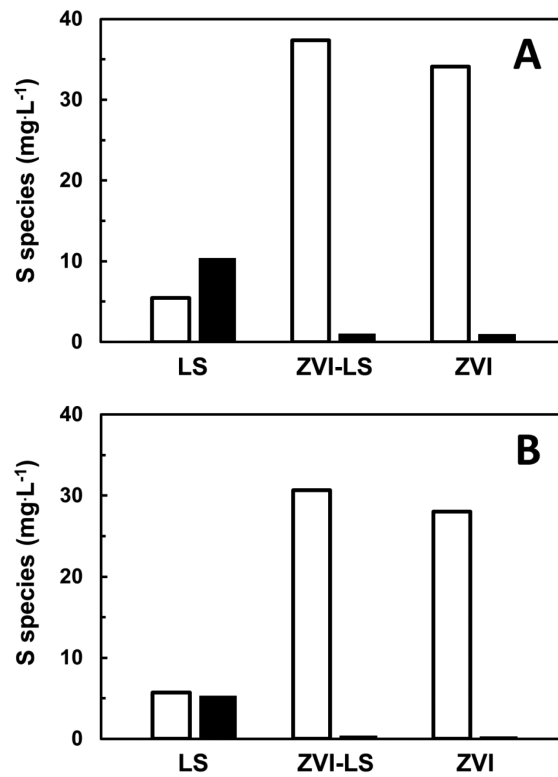


Fig. 6. Sulfide sequestered by the various bioreactors during two different experimental periods. Panel A represents the period from day 70 to 110 with no copper addition, and panel B represents the period from day 140 to 170 with copper addition of 10 mg L⁻¹. Sulfate removed (open bars) and sulfide discharged with effluent (filled bars).

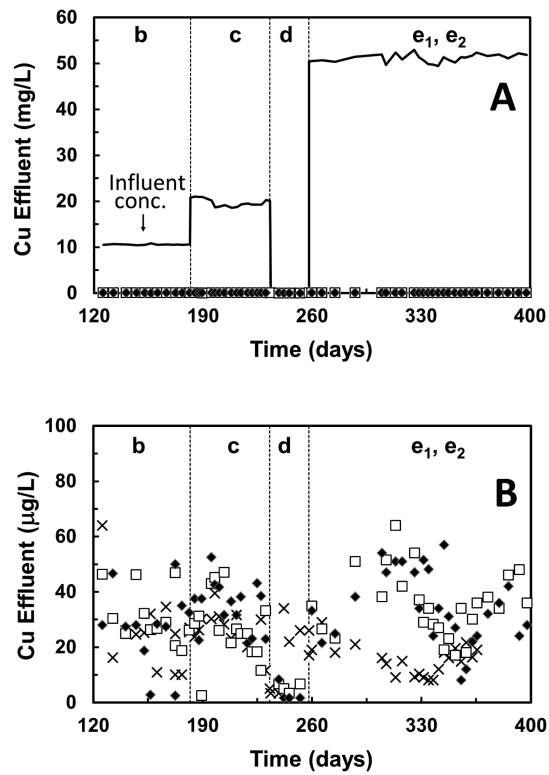


Fig. 7. Copper concentrations in the effluent of ZVI-LS column (◆), ZVI column (□), and LS column (×) during four periods based on influent copper concentrations ($\mu\text{g L}^{-1}$): 10,000 (b), 20,000 (c), 0 (d) and 50,000 (e). Panel A shows the complete results. Panel B zooms to $100 \mu\text{g L}^{-1}$ to visualize copper concentrations discharged from the columns.

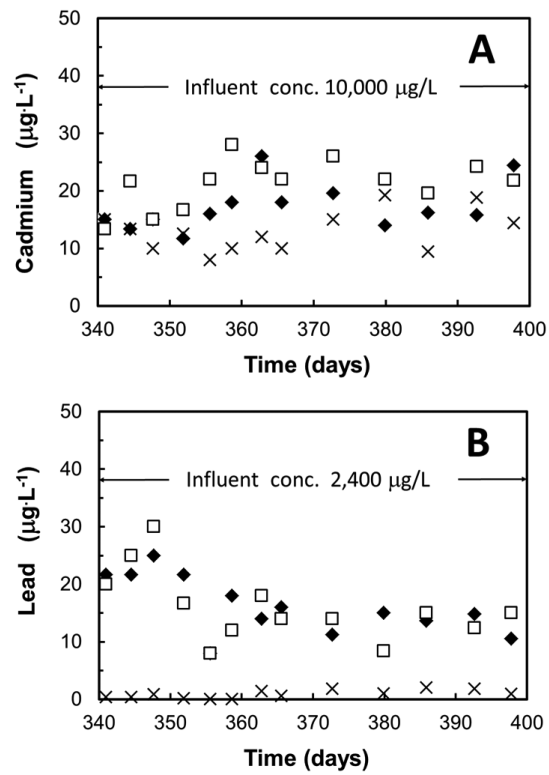


Fig. 8. Concentrations of cadmium (A) and lead (B) in the effluent of the ZVI-LS column (◆), ZVI column (□), and LS column (×) during the last period of operation, e_2 , of the with an influent containing $10,000 \mu\text{g Cd L}^{-1}$, $2,400 \mu\text{g Pb L}^{-1}$, and $50,000 \mu\text{g Cu L}^{-1}$.

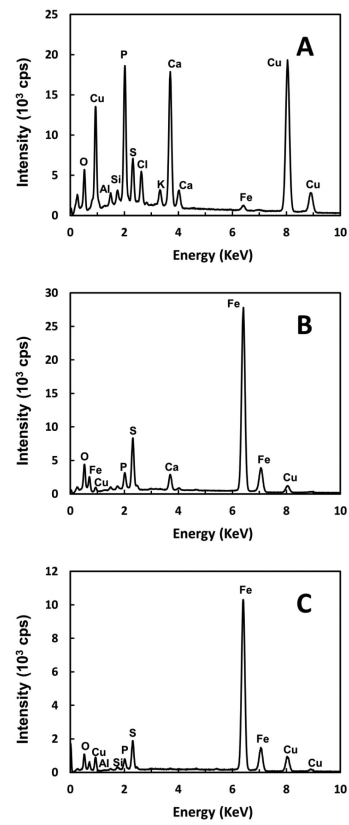


Fig. 9. SEM-EDS spectra of the packing in the LS column (A), ZVI-LS column (B), and ZVI column (C).

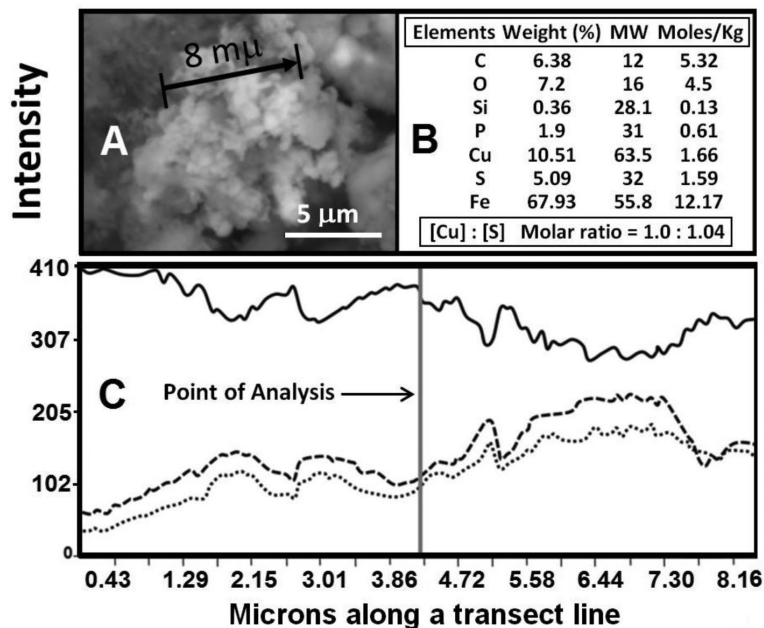


Fig. 10. SEM-EDS micrographs (A) and elemental composition (B) of an aggregate of Cu-sulfide in the packing of the ZVI-LS column. Panel C: Correlation of the intensities among Fe, Cu and S for the aggregate along the transect line. Fe (—), S (---) and Cu (....).

Table 1

Solubility products (K_{sp}) at 25°C of sulfides, carbonates and hydroxides of Cu²⁺, Cd²⁺, Pb²⁺ and Fe²⁺ [56].

Metal ion	Metal sulfide	Metal hydroxide	Metal carbonate
Cu²⁺	6.3×10 ⁻³⁶	2.5×10 ⁻¹⁹	3.1×10 ⁻¹²
Pb²⁺	1.0×10 ⁻²⁷	7.9×10 ⁻¹⁷	7.9×10 ⁻¹⁴
Cd²⁺	7.9×10 ⁻²⁷	2.5×10 ⁻¹⁴	1.0×10 ⁻¹²
Fe²⁺	6.3×10 ⁻¹⁸	7.9×10 ⁻¹⁵	3.5×10 ⁻¹¹

Author Manuscript

Author Manuscript

Author Manuscript

Author Manuscript

Table 2

Composition of the packing of the three continuous-flow columns utilized in this study.

Component ⁺	Columns*											
	LS				ZVI-LS				ZVI			
	DBD ^{**}	mass [‡] (g)	V/V [‡] (%)	mass (g)	mass (%)	V/V (%)	mass (g)	mass (%)	V/V (%)	mass (g)	mass (%)	V/V (%)
Limestone	1.50	183.6	36.5	36.9	183.6	31.5	36.8	0	0	0	0	0
Sand	1.53	320.0	63.5	63.1	215.0	36.9	42.2	400.0	68.6	78.9		
ZVI	2.62	0	0	0	183.4	31.5	21.0	183.4	31.4	21.1		

Notes:

* Packing volume (0.335 L).

** DBD = dry weight bulk density (g cm^{-3}).

[‡] V = volume.

[‡] Mass is provided in dwt.

⁺ The composition shown in Table 2 does not include the addition of sludge inoculum (54 g wet sludge or 4.16 g dwt sludge).

Table 3

Copper recovered by sequential extraction of the packing in different section of the up-flow columns: top (T), medium (M) and bottom (B).

Columns	Sections	Copper Extracted (%)			Copper Recovered (mg)		Removed (mg) [‡]	Recovery (%) ^{&}
		H ₂ O	HCl [*]	HNO ₃ /HCl [‡]	Section	Column		
LS	T	0.28	98.7	0	207			
	M	0.10	99.8	0.13	523	1383	1483	93
	B	0.07	99.8	0.09	653			
ZVI-LS	T	0	0.0	100	1.6			
	M	0	0.0	100	29.4	1254	1423	88
	B	0	0.05	99.9	1223			
ZVI	T	0	0.0	100	2.1			
	M	0	0.0	100	13.1	1087	1292	84
	B	0	0.27	99.7	1072			

Notes:

^{*} 1 M HCl

[‡] HNO₃-HCl, (3:1 v/v); 16 M and 12 M, respectively.

[‡] Cumulative copper removal calculated from difference between flux in and flux out.

[&] % Recovery = 100 × (copper extracted from packing material/cumulative copper removed).